Reinterpretation of Polypyrrole Electrochemistry after Consideration of Conformational Relaxation Processes

ARTICLE *in* THE JOURNAL OF PHYSICAL CHEMISTRY B · MAY 1997

Impact Factor: 3.3 · DOI: 10.1021/jp9630277

Reinterpretation of Polypyrrole Electrochemistry after Consideration of Conformational Relaxation Processes

Toribio F. Otero,* Hans-Jürgen Grande, and Javier Rodríguez

Laboratorio de Electroquímica, Facultad de Química, Universidad del País Vasco, P.O. Box 1072, 20080 San Sebastián, Spain

Received: October 2, 1996[⊗]

A simple model of polymeric relaxation, associated with the electrochemical switching of polypyrrole films between their reduced (insulating) and oxidized (electronically conducting) states, offers a reasonably precise description of the form of chronoamperograms obtained after previous subjection of the polymer film to cathodic potentials (which control the compactness of the neutral polymer) for long periods of time. The opening of the structure driven by the anodic potential is not uniform: nucleation of conducting zones inside the neutral polymer and their overlap at long times of anodic polarization are taken into account in the model. Diffusion of counterions from the solution across the oxidized zones is also included. The definition of a relaxation time (depending on both cathodic and anodic overpotentials and on temperature), and the inclusion of nucleation and diffusion processes, allows a theoretical simulation of chronoamperograms, in good agreement with experimental results from potential steps performed by changing the anodic and cathodic limits or at different temperatures.

1. Introduction

Polypyrrole conductivity can be enhanced by several orders of magnitude by passing from a neutral (or undoped) to a charged (or doped) state.[1] This doping process can be achieved by chemical or electrochemical methods, giving nonstoichiometric ionic compounds. In particular, the electrochemical way allows a perfect control of the attained doping level, so any intermediate composition can be attained: the weight percentage of counterions [A^-] and solvent [S] in the polymer [P] can be electrochemically changed in a continuous way from zero to about 50%, depending on both the electric potential applied to the polymer and the polarization time.[2] The doping process can be considered as a reversible redox reaction in the solid state which is summarized, in an oversimplified form, as

$$[P]_{solid} + n\{[A^-][S]_m\}_{solution} \underset{reduction}{\overset{oxidation}{\rightleftharpoons}} \{[P^{n+}][A^-]_n[S]_{n\cdot m}\}_{solid} + ne^- \quad (1)$$

Several theoretical models for explaining the electrochemical behavior of conducting polymers are available in literature. The most simple treatments focus on the role of penetrating counterions in the electrochemical switching of conducting polymers. In this sense, experimental data can be analyzed using a diffusion model (Cottrell equation) or, more adequately, by means of a migration model, e.g., the single-pore model of porous electrodes proposed by Posey and Morozumi.[3] Aoki and Tezuka[4,5] simulated chronoamperometric and voltammetric oxidation curves relying on the supposition that the conductive domain propagates from the metal−polymer interface to the polymer−solution interface. Feldberg[6] introduces capacitive currents to explain the form of voltammetric curves, making the assumption that the experimental value for the faradaic charge spent during complete oxidation of conducting polymers cannot be directly obtained from simple electrochemical experiments (e.g. cyclic voltammetry or chronoamperometry). Another type of model is based on the conservation of mass and charge along the different regions of the electrode. In this sense, White and co-workers[7,8] developed a mathematical model able to simulate cyclic voltammograms of polypyrrole on rotating disk electrodes. The polypyrrole film is treated as a porous electrode with a high surface to volume ratio and a large double layer capacitance, which is proportional to the amount of oxidized film, in a similar way to the model of Feldberg. Peter and co-workers[9] suggested that redox switching can be modeled in terms of an instantaneous twodimensional nucleation and growth model. Hillman et al.[10] pointed to the necessity of separating thermodynamic and kinetic phenomena during switching of electroactive polymer films. They propose a nonquantitative kinetic mechanism, consisting of a sequence of many elementary steps to produce regions of pure oxidized species from fully reduced regions. Finally, Kaplin[11] proposed a model for charge transfer controlled redox switching.

All of the abovementioned models assume that electrochemical responses of conducting polymers are unable to provide information about structural changes in the film. They do not take into account that conducting polymers films behave as three-dimensional electrodes; i.e., electrochemical processes occur throughout the film's volume, contrary to metallic electrodes where only the material situated at the metal−solution interface is electrochemically active. As result of this, electrochemical responses of conducting polymers have to follow not only electrochemical laws but are also subject to those features of structure and morphology common to amorphous polymer systems. Available models are based on simple electrochemical or geometrical aspects of the oxidation process, without any reference to structural features of the film, so only simple behaviors can be simulated. In this sense, studies pointing out the influence of the wait time at high cathodic potentials of prepolarization on the shape of anodic chronoamperograms[12,13] or voltammograms,[12−15] and the existence of first scan effects,[16,17] suggest that, under some special conditions, redox kinetics in conducting polymers can be driven by the rate at which structural changes in the solid matrix occur. The nature of those structural changes is under debate at present: cis−trans isomerizations in the polyconjugated chains,[18] variation

[⊗] Abstract published in *Advance ACS Abstracts,* April 15, 1997.

S1089-5647(96)03027-1 CCC: $14.00

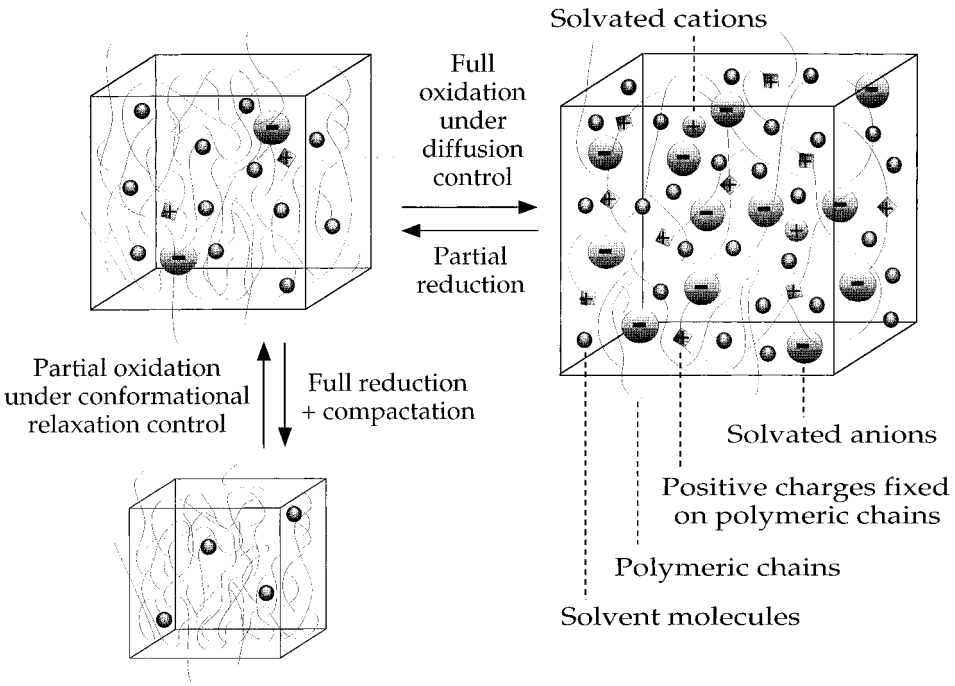

Figure 1. Schematic representation of the reversible variation of volume associated to the electrochemical switching of polypyrrole. Changes in free volume are mainly due to two effects: electrostatic repulsions between fixed positive charges and exchange of cations, anions, and solvent molecules between the polymer and the solution.

of equilibrium constants of polarons and bipolarons,[19] rearrangement of conducting clusters in electrical contact with the electrode,[20,21] cathodic annealing[22] or conformational changes giving variations in interchain free volume[12] have been proposed. In spite of experimental difficulties to follow structural changes at molecular level, many macroscopic prices of evidence point to conformational changes as being responsible for the observed anomalous effects in electrochemical behaviors.

Conformational changes here have to be considered as variations in the overall three-dimensional shape adopted by a polymeric segment by rotation around the single bonds present between consecutive pyrrole units in the neutral state. Those single bonds are progressively transformed to double bonds, and again to single bonds, when an increasing population of positive charges on the chains (polarons initially and bipolarons later) is achieved, leading to continous changes in the rotation angles.[23] As those transformations in the geometry of the chains are linked to an electrochemical reaction, they can be considered as electrochemically induced conformational changes. Associated variations in the interchain free volume will depend on the kind of interchain interactions prevailing in the polymer after an anodic disturbance. In neutral polypyrrole attractive interactions between neighboring chains prevail, resulting in a compact and closed polymer structure. As oxidation advances, polymer−polymer attractive forces are substituted by strong Coulombic repulsion forces between emerging polarons. Concomitant conformational movements of the polymer chains promote increasing interchain distances, allowing the generation of free volume which is immediately occupied by solvated counterions penetrating from the solution.[12,24−27] As consequence, the polypyrrole film volume increases greatly during oxidation (about 40−45%), as was experimentally demonstrated by several authors.[28,29] This behavior is schematically represented by Figure 1. Opposite processes occur during reduction, i.e., positive charges on the polymer are neutralized and counterions are expelled to the solution. Volume elements of the polymeric chains move into the free volume left by counterions, thus promoting the closure of the polymeric structure. Nevertheless, some authors[30−32] have detected an appreciable increase of volume in the first stages of reduction, which was attributed to the initial incorporation of cations from the electrolyte, followed by the diffusion of ion pairs from the neutral polymer (salt draining), resulting finally in an overall volume contraction with time. When polyanions or other immobile anions are used for doping, the mechanism involves the entrance of cations (and hence increase of volume) during reduction and their subsequent expulsion during oxidation.[33−35] Whatever the mechanism of redox switching is, macroscopic volume changes related to microscopic conformational movements during redox processes in polypyrrole films have been applied to the fabrication of electrochemomechanical devices as artificial muscles.[29,36−40]

According to this description, the most compact structure for a single redox process involving interchange of small and mobile anions has to be attained under total elimination of positive charges along the polymeric chains, that is, at very negative potentials (Figure 1). This structural feature may be seen in the electrochemical response of the polymer during redox cycling. In other words, starting from more cathodic potentials, extra energy will be required to open the compacted polymer network structure during oxidation before the entrance of counterions is allowed. Working under constant temperature, the only way to get energy is by means of an electric overpotential. Thus, increasing anodic potentials or higher times of anodic polarization are required to open more compact structures, which were closed at higher cathodic potentials. We believe that this extra energy is consumed by conformational changes required to generate an increase in polymeric free volume.

The aim of this work is to incorporate this structural information into a theoretical model, which will be able to predict the influence of different experimental variables (cathodic or anodic, potential limits, and temperature) on the shape of oxidation chronoamperograms (one of the more simple and easily treatable electrochemical responses) of polypyrrole films. Both electrochemical and structural values are included in a conformational relaxation time, which controls the rate of redox processes after closure of the polymeric structure under reduction conditions. Thus, our task is to develop an electrochemically

TABLE 1: Comparison between Different Relaxation Theories Available in Literature

relaxation theory	origin	action	response
electrochemical	structure closure under cathodic prepolarization	anodic potential step or scan	oxidation current
dielectric	polarization under electric field	temperature step or scan	depolarization current
mechanical	viscoelasticity	mechanical stress	deformation
magnetic	imanation under magnetic field	temperature step or scan	changes in magnetic properties

stimulated conformational relaxation model for conducting polymers, attempting to state the basis for an integration of polymer science and electrochemistry, as other relaxation models do in their respective fields (see Table 1). In future revisions, our model should be capable of quantifying and predicting changes in electrochemomechanical (artificial muscles, sensors, and actuators) and electrochromic (smart windows, filters, or mirrors) properties, as well as processes occurring in polymeric batteries, biological or artificial membranes, etc.

2. Experimental Section

Polypyrrole films were electropolymerized and checked in a one-compartment electrochemical cell, connected to a PAR M273 potentiostat−galvanostat and controlled by an IBM PS/2 computer. Working electrode and counterelectrode were platinum sheets having 1 and 4 cm^2 of surface area, respectively. A saturated calomel electrode (SCE) from Crison Instruments was used as reference electrode. Pyrrole (Jansen) was distilled under vacuum before use. Acetonitrile (Lab Scan, HPLC grade), propylene carbonate (Merck, >99% content), and anhydrous lithium perchlorate (Aldrich, 95% content) were used as received. All the solutions were deaerated by bubbling N_2 for 10 min before the current flow. The temperature of the cell was maintained constant with a Huber ministat.

Polypyrrole films were electrogenerated on a 1 cm^2 platinum sheet using acetonitrile, with a 2% of water content, as solvent, 0.1 M $LiClO_4$ as electrolyte, and 0.1 M pyrrole as monomer, by passing 120 mC at 800 mV vs SCE at room temperature. A polypyrrole film of about 0.22 μm of thickness was obtained, showing electrochromic properties (yellow in reduced state and blue when it was oxidized). After generation, the polymer-coated electrode was dried in air and transferred into the background solution (0.1 M $LiClO_4$ in dry propylene carbonate, without monomer), where it was subjected to chronoamperometric analysis. Before the realization of the potential steps, the electrode was reduced in the background solution at the selected potential for 2 min.

3. Results and Discussion

The occurrence of a progressive closure of the polymeric structure at increasing cathodic potentials of departure can be easily proved by electrochemical methods. Figure 2 shows the evolution of the reduction charge as a function of the applied potential during a negative potential sweep at a scan rate of 30 mV s^{-1}. As can be seen, even though most of the polymer becomes reduced at −900 mV, the charge remaining in the film decreases slowly and almost linearly with the cathodic potential below −900 mV. Voltammograms show that these does not exist a negative potential where the cathodic current becomes equal to zero (see onset on Figure 2). Cathodic currents are present even at −3000 mV, hence promoting a continuous closure and compacting of the polymeric structure during reduction, probably due to an electroosmotic effect. A similar effect was observed when a polypyrrole film was subjected to a constant cathodic potential.

The rate at which further oxidation occurs is influenced by the degree of compactness of the polymeric structure attained during reduction or, consequently, by the cathodic potential of

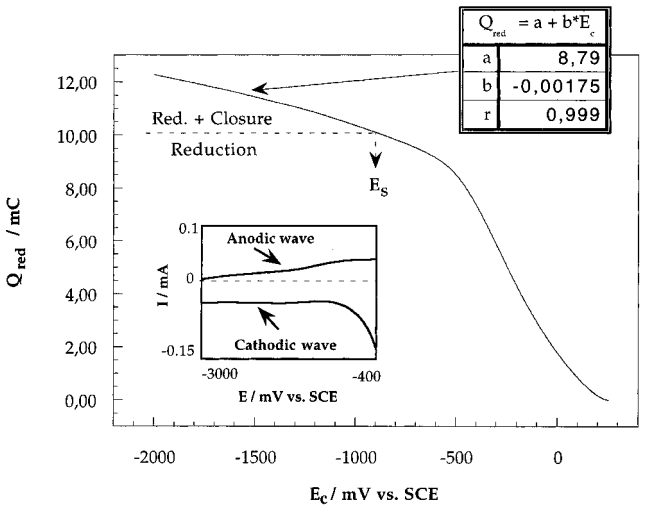

Figure 2. Evolution of the charge of reduction as a function of the applied potential during a cathodic potential scan for a polypyrrole film. The voltammogram was performed in a 0.1 M $LiClO_4$ propylene carbonate solution at 30 mV/s. The onset on the figure shows the evolution of both oxidation and reduction currents at very low cathodic potentials.

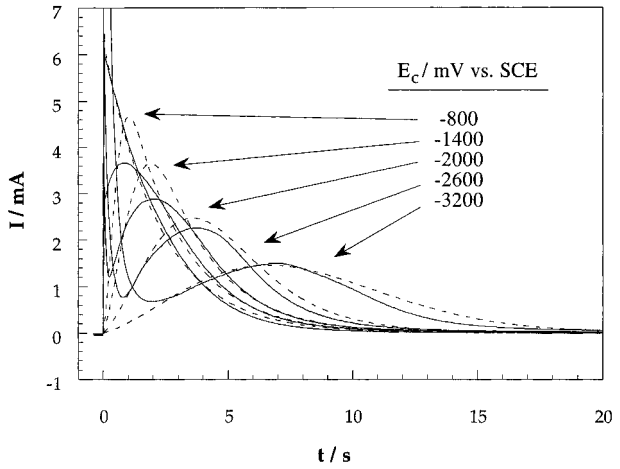

Figure 3. Experimental (—) and theoretical (- - -) chronoamperometric responses to potential steps carried out on a polypyrrole electrode in a 0.1 M $LiClO_4$ propylene carbonate solution from different cathodic potentials, indicated on the figure, to 300 mV vs. SCE.

departure. This influence is illustrated in Figure 3 (solid lines), which shows experimental chronoamperograms performed from different cathodic potentials (ranging between −3200 and −800 mV) to the same anodic limit (300 mV) at room temperature (25 °C). When the polymer film was prepolarized at −800 mV, the subsequent potential step gives a continuous decrease of the current density, after a sharp initial peak related to the charge of the electrical double layers. The shape of this curve is that of a counterion diffusion-controlled process,[3] thus showing that the compaction of the polymeric structure, able to control the rate of subsequent oxidation, only happens at potentials more cathodic than about −900 mV. In fact, chronoamperograms performed from more cathodic potentials show, besides the initial charging of the double layers, a slow increase in current linked to the relaxation process, pointing to an oxidation initiated

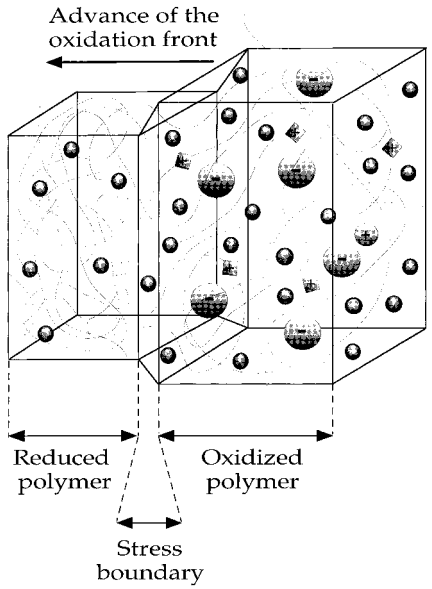

Figure 4. Evolution of the structure and composition of polypyrrole during electrochemical oxidation. Reduced and partially oxidized regions coexist with zones where the polymer is being relaxed. Relaxation-controlled oxidation occurs on the borders between oxidized and reduced regions and full oxidation under diffusion control takes place in the bulk oxidized material.

from different nuclei on the film surface, followed by a maximum related to the coalescence between the different expanding regions of oxidized polymer. At long times of anodic polarization, once the chronoamperometric maximum was reached, the intensity follows a first-order decay which can be attributed to a diffusion-controlled process.

From those experimental observations, it can be stated that in polypyrrole films whose structure was closed under cathodic prepolarization, the oxidation mechanism changes in relation to films having a more opened structure: oxidation (and therefore the swelling of the polymeric structure) is initiated on singular points which expand like in pitting corrosion processes of metals.[12] As the polymer structure is now compact, counterions cannot penetrate inside the polymer, and thus electrogenerated positive charges concentrate on the polymer surface where they can be compensated by counterions present in the solution. Nevertheless, at specific points of the film surface where irregularities exist (irregularity here means free cooperative chain motions), the penetration of counterions (having a diameter of about 3.5 Å) inside the polymer is favored. Those points actuate like nucleation points for the oxidation of the polymer. Mechanical stresses, appearing on the borders between the oxidized regions and the neutral film (see Figure 4), favor further conformational relaxation processes, so the nuclei have a tendency to expand like hemispheres inside the reduced film.[29] However, due to the increase of the potential gradient between the nuclei and the electrode, the oxidation boundary progresses faster toward the metal−polymer interface. Thus, columns of conducting material are formed, which expand on the film until their coalescence. The generation and growth of oxidation nuclei can be well observed when thin and electrochromic polypyrrole films are formed on polished platinum surfaces (Figure 5). The number of nuclei can be well determined (5−9 per cm^2), and it can be seen how blue circles of oxidized polypyrrole expand across a yellow reduced film during the switching process.

Not only the shape of the chronoamperograms but also the position of the maxima changes as consequence of structural effects. Longer times for the maxima and lower current densities are obtained after prepolarization from more negative potentials. That indicates that more compact structures were obtained at the beginning of the oxidation when the potential

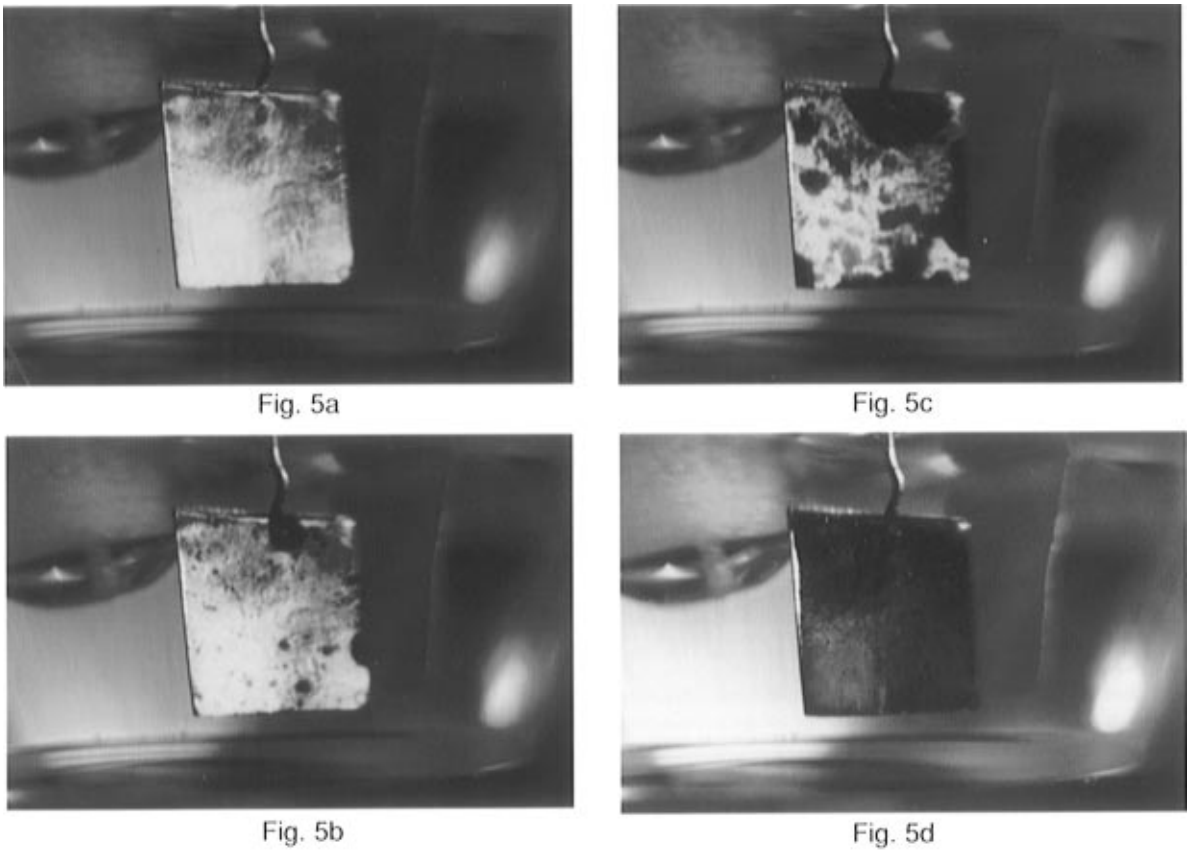

Figure 5. Photographs of a mirror polished platinum electrode coated with an electrochromic polypyrrole film, when it was (a) fully reduced, (b,c) partially oxidized, and (d) fully oxidized after an anodic potential step from −2000 to 300 mV in a 0.1 M $LiClO_4$ propylene carbonate solution.

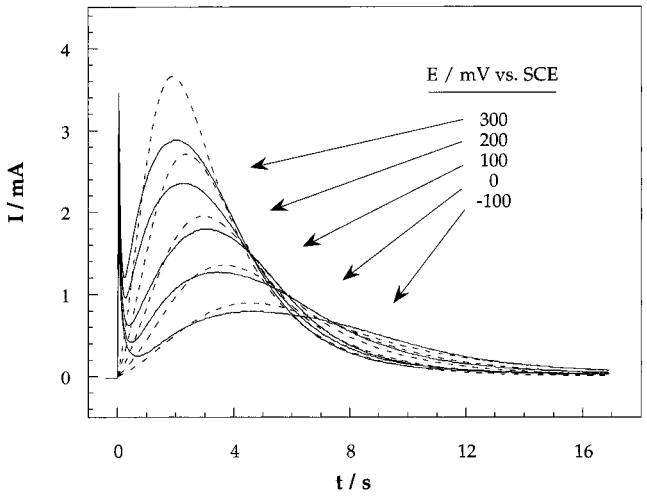

Figure 6. Experimental (—) and theoretical (- - -) chronoamperometric responses to potential steps carried out on a polypyrrole electrode, in a 0.1 M $LiClO_4$ propylene carbonate solution, from −2000 mV to different anodic limits, which are indicated on the figure.

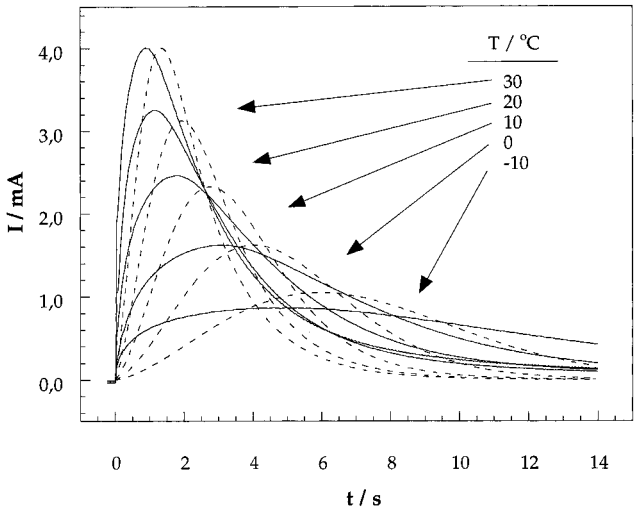

Figure 7. Experimental (—) and theoretical (- - -) chronoamperometric responses to the application of potential steps from −2000 to 300 mV in a 0.1 M $LiClO_4$ propylene carbonate solution, at different temperatures indicated on the figure. Cathodic prepolarization temperature was always 25 °C (room temperature).

of prepolarization was more cathodic and, hence, greater times and energies were required to allow conformational movements.

Similar results are obtained when other experimental variables were changed. Curves for potential steps performed from −2000 mV vs SCE, which was maintained for about 2 min each time, until different anodic potentials (ranging between −100 and 300 mV) are depicted by Figure 6 (solid line). Times required to attain the maxima are shorter at increasing anodic potentials, revealing that conformational relaxation processes are as faster as more energy is given to chains through anodic overpotentials. We interpret these results to mean that conformational changes in conducting polymers can be driven by electric fields.

Another way to supply energy to the polymer chains in order to promote faster conformational changes is by increasing temperature. With the aim of studying the influence of temperature on the oxidation rate, a polypyrrole-coated platinum electrode was reduced and compacted by cathodic polarization at −2000 mV in a 0.1M $LiClO_4$ propylene carbonate solution at 25 °C for 2 min. The electrode was then extracted from the background solution and maintained in N_2 gas above the solution; meanwhile the temperature of the solution was regulated to a new value, in the range between −10 and 30 °C. The compacted and reduced electrode was again immersed in the solution and subjected to a potential step from −2000 mV (0.1 s) to 300 mV during 20 s. The same procedure was repeated changing the oxidation temperature each time. As the polymer is reduced every time under the same experimental conditions (cathodic potential, temperature and time), the compactness attained during reduction is also the same. Thus, when the polymer is later subjected to the same anodic step at different temperatures, the experimental changes observed on the oxidation rates (see Figure 7, solid line) will be only due to differences in the thermal energy available by the polymeric segments to undergo conformational changes. As expected, conformational relaxation occurs faster at increasing temperatures, promoting a shift of the chronoamperometric maxima toward lower times. This evolution is similar to that observed above for increasing anodic potential limits. Higher energies available by the polymeric segments promote, in both cases, faster conformational changes and, hence, shorter times until the coalescence between the oxidation nuclei is completed.

4. Theoretical Section

Experimental results allow to divide the oxidation process into four steps:

1. Electron loss from the polymer chains, with formation of polarons (radical cations) and bipolarons (dications).
2. Conformational relaxation of the polymer chains with generation of free volume, being the process initiated from surface nuclei: relaxation−nucleation process.
3. Exchange of counterions between the polymer and the solution in order to keep the electroneutrality in the film: counterion diffusion process.
4. Additional exchange of ion pairs (salt draining) and solvent molecules.

Most of theoretical approaches available in literature consider the electron loss or the counterions diffusion as rate-limiting steps. Instantaneous two-dimensional nucleation processes have also been considered. Our approach, however, will rely on the hypothesis of a conformational relaxation control for the nucleated oxidation process. Changes in the oxidation rate referred to above have been related to a higher compactness of the polymer structure attained along cathodic prepolarization and to a higher energy (coming from thermal or electrochemical sources) required by polymeric chains to undergo conformational changes along further oxidation. Once the opening of the polymeric structure is completed, we assume the oxidation to be completed under the control of diffusion laws. So both structural and electrochemical magnitudes have to be included in a theoretical model attempting to explain those experimental results.

Conformational Relaxation Time. After an anodic potential step initiated from a compact polymeric structure, oxidation only can occur when conformational movements of chains allow the penetration of counterions. This is a conformational relaxation process, which can be quantified through a conformational relaxation model. To develop an electrochemical theory of conformational relaxation we have to define a relaxation time (τ) as the time required to change the conformation of a polymeric segment, previously subjected to a cathodic potential E_c, when it is oxidized to an anodic potential E. A polymeric segment is considered as the minimum chain length whose conformational changes allow ionic interchanges between the polymer and the solution. The relaxation time is related to the

change in the molar conformational free energy (ΔH) by an Arrhenius law:

$$\tau = \tau_0 \exp(\Delta H/RT) \tag{2}$$

Equation 2 is the same whatever the relaxation theory. In our model of electrochemically stimulated conformational relaxation, ΔH can be expressed as the sum of three terms:

$$\Delta H = \Delta H^* + \Delta H_c - \Delta H_e \tag{3}$$

where ΔH^* is a mechanical component, defined as the conformational energy consumed per mole of polymeric segments in absence of any external electric field, ΔH_c represents the increment in conformational energy arisen from the closure of the polymeric matrix during cathodic polarization, and ΔH_e includes the decrease in conformational energy due to the application of an anodic potential to the reduced polymer. The closure of the polymeric matrix can be assumed to be proportional to a cathodic overpotential (η_c), related to the potential at which the polymer structure closes along a negative potential sweep (E_s). Under our simplified model, that means that starting from a potential more anodic than E_s the oxidation will not be controlled by energetic requirements to open the polymeric network, but by counterion diffusion along the open structure. However, starting from a potential more cathodic than E_s, an extra energy is required to open the polymeric structure (just ΔH_c) before the diffusion of counterions is allowed: the electrochemical reaction is under conformational relaxation control. So ΔH_c is the minimum energy required to allow counterions penetration after cathodic prepolarization. The relationship between ΔH_c and the cathodic overpotential can be summarized as

$$\Delta H_c = z_c \eta_c = z_c(E_s - E_c) \tag{4}$$

where z_c, defined as the coefficient of cathodic polarization, is related to the charge required to compact one mole of polymeric segments.

On the other hand, the energy needed to relax one mol of polymeric segments decreases in a value equal to ΔH_e when an anodic overpotential is applied to the polymer. As the oxidation level (the number of charges consumed to oxidize a polymeric segment) depends on the applied potential, this electrochemical energy will be proportional to the anodic overvoltage (η):

$$\Delta H_e = z_r \eta = z_r(E - E_o) \tag{5}$$

where z_r is the coefficient of electrochemical relaxation, which is related to the charge needed to relax one mole of polymeric segments, and E_o is the oxidation potential of the conducting polymer.

Thus the relaxation time becomes

$$\tau = \tau_0 \exp[(\Delta H^* + z_c \eta_c - z_r \eta)/RT] \tag{6}$$

Equation 6 includes magnitudes related to the polymeric structure (as τ_0, ΔH^*, and z_c) together with electrochemical magnitudes (T, z_r, η, and η_c). So features concerning electrochemistry and polymer science can be integrated in a single equation describing the rate of oxidation of a polymeric segment previously subjected to cathodic prepolarization. In order to simplify the mathematical treatment, henceforth we will make use of eq 2 in our description, but it must not be forgotten that ΔH depends on both anodic and cathodic overpotentials.

Nucleation and Expansion of Conducting Regions. Once formed, the columns of oxidized polymer begin to expand, this process being controlled by conformational relaxation in the borders between the oxidized and reduced regions. In order to advance in the development of our model by the inclusion of this process, the following simplifications and hypothesis were considered:

1. N_o nuclei per cm^{-2} appear at the beginning of the oxidation process, being constant both temperature and electrolyte concentration in a specific solvent.
2. Relaxation nuclei expand concentrically as cylinders until their coalescence.
3. Along this time oxidized and neutral phases coexist, having clear separation surfaces (i.e., the lateral area of the cylinders).
4. Oxidized regions are uniform in composition and, subsequently, in charge density at every polarization time. Regions of neutral polymer have, as well, a uniform composition. Both oxidized and neutral regions have an amorphous structure.
5. The relaxation of a mole of segments on the oxidized/neutral polymer borders involves the loss of q_r electrons and the subsequent storage of q_r positive charges. At the same time, q_r solvated monovalent anions penetrate into the polymer from the solution.
6. The relaxation of an elemental segment is completed after a time t. This assumption approaches the relaxation process to a step function.
7. The overall charge (Q_t) consumed to oxidize the film by a potential step from E_c to E has two components: the charge consumed to relax the compact structure, which will be named relaxation charge (Q_r), and the charge consumed under diffusional control to complete the oxidation, named ahead diffusion charge (Q_d). The following equation is obeyed:

$$Q_t = Q_r + Q_d \tag{7}$$

Capacitive charges are neglected in this approach.

Under those conditions, it can be stated that the radius of the cylinders increases by a length λ in a time τ, λ and τ being the length and relaxation time of a single polymeric segment, respectively:

$$\frac{dr}{dt} = \frac{\lambda}{\tau} = \frac{\lambda}{\tau_0} \exp[-\Delta H/RT] \tag{8}$$

And by integration

$$r = (\lambda/\tau_0) \exp[-\Delta H/RT]t \tag{9}$$

That means a constant expansion rate of each cylinder along the polarization time. The expansion rate decreases for increasing cathodic potentials of prepolarization, for decreasing anodic potentials, or for decreasing step temperatures, in good agreement with experimental results as will be shown later.

In order to obtain the current consumed along the nucleated relaxation process under a constant potential, we consider that a stationary density of charge (δ_t) will be stored in the polymer. The storage of those charges is controlled by both conformational relaxation (δ_r) and diffusion (δ_d) processes, so

$$\delta_t = \delta_r + \delta_d \tag{10}$$

All those densities are related to the volume (V) of the film, given by

$$V = Ah \tag{11}$$

h being the thickness of the polymer film and *A* the area of the polymer−solution interface.

The surface concentration of polymeric segments being relaxed by conformational movements on the borders of the oxidized regions (σ) can be expressed as follows:

$$\sigma = \delta_r \lambda / q_r \tag{12}$$

The amount of polymeric segments relaxing on the borders of the expanding cylinders by unit of time and unit of area (k) can be obtained by dividing eq 11 by the relaxation time (τ):

$$k = \delta_r \lambda / q_r \tau \tag{13}$$

If h is the height of every cylinder (i.e., the thickness of the polymer film) which expansion follows eq 8, the current associated to the relaxation controlled oxidation $I_r(t)$ in the borders of the cylinder can be stated as

$$I_r(t) = 2\pi r h q_r k = 2\pi r h \delta_r (\lambda/\tau) \tag{14}$$

Equation 14 can be modified by application of eqs 2, 9, and 11 and by considering that N_o nuclei are growing simultaneously:

$$I_r(t) = \frac{2\pi N_o \lambda^2}{\tau_0^{\,2} A} Q_r \exp[-2\Delta H/RT] t \tag{15}$$

Coalescence between Conducting Regions. Equation 15 works until coalescence between adjacent nuclei starts. Considering the symmetry of the growing process, our three-dimensional system is reduced to a problem of two dimensions, so Avrami's treatment can be applied:[41−43]

$$I_r(t) = I_{ext} e^{-S_{ext}} \tag{16}$$

Here $I_r(t)$ is the electrical current flowing after coalescence, I_{ext} is the extended value of intensity given by eq 15, and S_{ext} is the extended oxidation area without considering the existence of coalescence, referenced to the total film area (A). The value of S_{ext} can be easily deduced from eq 9:

$$S_{ext} = \frac{\pi N_o \lambda^2}{\tau_0^{\,2} A} \exp[-2\Delta H/RT] t^2 \tag{17}$$

Final Equations for the Relaxation Controlled Oxidation. Taking into account the coalescence between the oxidized regions along the oxidized zones, the final equation for the current intensity becomes

$$I_r(t) = \frac{2\pi N_o \lambda^2}{\tau_0^{\,2} A} Q_r \exp[-2\Delta H/RT] t \times \exp\left[-\frac{\pi N_o \lambda^2}{\tau_0^{\,2} A} \exp[-2\Delta H/RT] t^2\right] \tag{18}$$

The consumed relaxation charge is obtained by integration along the polarization time:

$$Q_r(t) = Q_r\left[1 - \exp\left[-\frac{\pi N_o \lambda^2}{\tau_0^{\,2} A} \exp[-2\Delta H/RT] t^2\right]\right] \tag{19}$$

Equations 18 and 19 give the shape of theoretical chronoamperograms and cronocoulograms obtained when a conducting polymer film is submitted to a potential step from an initial potential E_c (more cathodic than E_s) to an anodic value E. They include structural magnitudes of the polymer, as the length of an elemental segment (λ), the number of nucleus under defined experimental conditions (N_o), the preexponential factor of the relaxation time (τ_0), the cathodic polarization coefficient (z_c), and the conformational energy in absence of external electric fields (ΔH^*). They also contain geometrical variables as the area of the polymer film (A), and electrochemical magnitudes as cathodic (η_c) and anodic (η) overpotentials, the relaxation charge (Q_r), the electrochemical relaxation coefficient (z_r), and the temperature (T). All those magnitudes can be determined experimentally, and only λ/τ_0 has to be estimated.

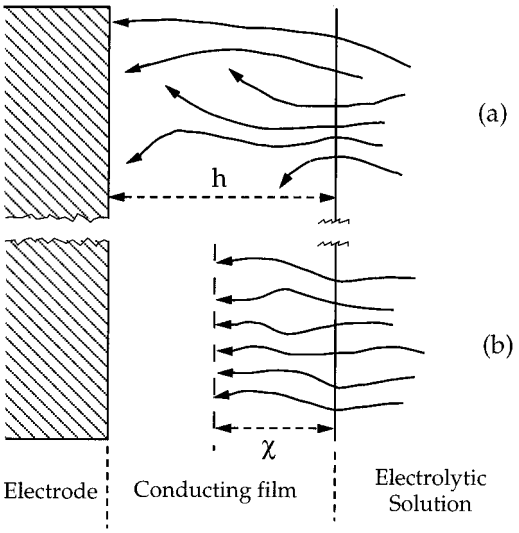

Figure 8. Lateral section of the polymeric film once the opening of the polymeric structure is completed, showing that the transport of counterions across the solid matrix (a) can be simplified to an unidimensional diffusion across a length χ (b).

The relaxed area is given by eq 20 as a function of polarization time. This result will be used later:

$$A(t) = A\left[1 - \exp\left[-\frac{\pi N_o \lambda^2}{\tau_0^{\,2} A} \exp[-2\Delta H/RT] t^2\right]\right] \tag{20}$$

The obtained expressions can be better examined when a new parameter a is defined:

$$a = \frac{\pi N_o \lambda^2}{\tau_0^{\,2} A} \exp[-2\Delta H/RT] \tag{21}$$

So eqs 18, 19, and 20 become:

$$I_r(t) = 2atQ_r \exp(-at^2) \tag{22}$$

$$Q_r(t) = Q_r[1 - \exp(-at^2)] \tag{23}$$

$$A(t) = A[1 - \exp(-at^2)] \tag{24}$$

Diffusion-Controlled Full Oxidation. As has been pointed out above, when the relaxation of the polymer has been initiated and the oxidized zones are growing, a second process is present: the transport of counterions across the solid polymer in order to complete the oxidation of the previously relaxed polymer. This process can be separated into two parts: transport through the polymer−solution double layer and diffusion through the oxidized polymer toward the oxidation centers (Figure 8a). This last component can be considered the rate-controlling step, so we will focus on its description. For

simplicity, the flow of ions into the polymer ($F(t)$) can be assumed to be proportional to the difference between the diffusion charge density in the oxidized regions when the film attains the oxidation steady state at large polarization times (δ_d) and the charge density stored after a given polarization time ($\delta_d(t)$):

$$F(t) = D[\delta_d - \delta_d(t)]/\chi \tag{25}$$

where D is the diffusion coefficient of counterions in the solid polymer (it is a function of temperature, anodic potential, and both nature and concentration of the electrolyte in the solution) and χ is the equivalent diffusion length across the polymer, which value can be approached to $h/2$ (Figure 8b). An infinitesimal fraction of the polymer will be considered, consisting of all the segments which are relaxed at the same time (t'). As result of the flow given by eq 25, the increment of charge stored under diffusion control ($dQ_d(t)$) in this infinitesimal portion of the polymer at a given time $t > t'$ will be given by:

$$dQ_d(t) = dQ_d\left[1 - \exp\left(-\frac{2D(t-t')}{h^2}\right)\right] \tag{26}$$

which can be simplified by the introduction of a new parameter b, expressed as

$$b = 2D/h^2 \tag{27}$$

In eq 26, dQ_d is the overall diffusion charge for the segments relaxed at a time t'. Its value can be related to the infinitesimal increment in the area of the conducting regions between t' and $t' + dt'$, according to eq 24:

$$dQ_d = Q_d \frac{dA(t')}{A} = 2aQ_d t' \exp(-at'^2)\, dt' \tag{28}$$

With those modifications, eq 26 becomes

$$dQ_d(t) = 2aQ_d t' \exp(-at'^2)[1 - \exp[-b(t-t')]]\, dt' \tag{29}$$

The integration of eq 29 yields the diffusion charge consumed until a given time in those regions where the structure was opened:

$$Q_d(t) = Q_d[1 - \exp(-at^2) - 2a \exp(-bt) \times \int_0^t t' \exp(bt' - at'^2)\, dt'] \tag{30}$$

The current flowing through the electrode due to diffusion-controlled oxidation can be easily deduced from eq 30:

$$I_d(t) = 2abQ_d \exp(-bt) \int_0^t t' \exp(bt' - at'^2)\, dt' \tag{31}$$

If the polymeric structure is open at the beginning of the oxidation, t' becomes equal to zero for every segment. So equations for charge and intensity turn to

$$Q_d(t) = Q_d\,[1 - \exp(-bt)] \tag{32}$$

$$I_d(t) = bQ_d \exp(-bt) \tag{33}$$

Equation 32 can be represented in a linear form, which allows the obtention of parameter b, and its evolution as a function of the different electrochemical variables, from experimental data:

$$\ln\left[1 - \frac{Q_d(t)}{Q_d}\right] = -bt \tag{34}$$

Theoretical Chronoamperograms and Chronocoulograms. Equations 30 and 31, joined to eqs 22 and 23, define the electrochemical oxidation process of a conducting polymer film controlled by conformational relaxation and diffusion processes in the polymeric structure. It must be remarked that, if the initial potential is more anodic than E_s, then the term depending on the cathodic overpotential vanishes and the oxidation process becomes only diffusion controlled. So, the most usual oxidation processes studied in conducting polymers, which are controlled by diffusion of counterions in the polymer, can be considered as a particular case of a more general model of oxidation under conformational relaxation control. The addition of relaxation and diffusion components provides a complete description of the shapes of chronocoulograms and chronoamperograms in any experimental conditions:

$$Q(t) = (Q_r + Q_d)\,[1 - \exp(-at^2)] - 2aQ_d \times \exp(-bt) \int_0^t t' \exp(bt' - at'^2)\, dt' \tag{35}$$

$$I(t) = 2aQ_r t \exp(-at^2) + 2abQ_d \exp(-bt) \times \int_0^t t' \exp(bt' - at'^2)\, dt' \tag{36}$$

Those equations describe the polymer oxidation as a function of electrochemical and structural variables. So our simplified model has opened a way to integrate both polymer science and electrochemistry in a single model. In the following section, the ability of our model to predict experimental responses to potential steps and their dependence on different experimental variables will be checked.

5. Simulation

Modeling of oxidation processes in conducting polymers from a conformational relaxation point of view (that is, following eq 22) provides a good way to study the influence of different electrochemical variables on the position of the chronoamperometric maxima, as reported in previous works.[44,45] However, in order to achieve theoretical simulations of chronoamperograms it is necessary to include not only the electrical current required to relax the polymeric structure by conformational movements but also the current involved to charge the electrical double layers and that required to complete the oxidation process by diffusion control once the structure is opened. As referred to above, charges related to initial processes after the potential steps, like charging of the metal−polymer and polymer−solution double layers, are not considered in this work, so eq 36 fulfills our initial requirements.

A polypyrrole thin film having 0.22 μm of thickness and 1 cm^2 of surface area was considered. Experimental magnitudes related to this film and required to solve eq 36 are $E_s = -900$ mV,[44] $E_o = -550$ mV vs SCE,[45] $N_o = 7$,[45] $z_c = 4600$ C mol^{-1},[44] $z_r = 3650 + 1.827(E_s - E_c)$ C mol^{-1},[44] and $\Delta H^* = 27\,500$ J.[46] The overall electrical charge stored in the polymer film was probed to be a linear function of the applied anodic potential: $Q(E) = 9.362 + 0.0156E$ (where the charge is expressed in mC and the anodic potential in mV). This empirical relationship was experimentally deduced from the integration of experimental curves in Figure 6. Otherwise, it was observed that the rate at which intensity decays in a diffusion-controlled oxidation process is mainly dependent on the applied anodic potential, According to eq 34, a semilogarithmic plot of $(1 - Q_d(t)/Q_d)$

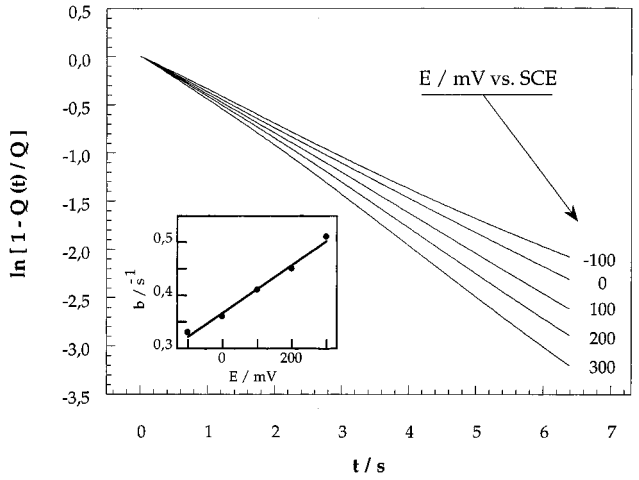

Figure 9. Semilogarithmic plot of $1 - Q(t)/Q$ vs oxidation time for a series of potential steps performed from −800 mV to different anodic values indicated on the figure. Values of the diffusional parameter b were obtained from the slopes for the different applied anodic potentials.

vs polarization time for potential steps performed from −800 mV (at which the polymer structure remains open) to different anodic limits (see Figure 9) allows us to obtain the parameter b as a function of the applied anodic potential: $b = 0.367 + 0.000\,45E$ (in s^{-1}). Those values can be translated into diffusion coefficients (D), giving values ranging between 1.0×10^{-10} $cm^2\ s^{-1}$ at 300 mV and 6.6×10^{-9} $cm^2\ s^{-1}$ at −100 mV vs. SCE. Those are usual values for diffusion processes in solid state. On the other hand, considering a symmetric redox process, the ratio between the relaxation charge (Q_r) and the overall oxidation charge (Q) can be assumed to be equal to the ratio between the charge spent in the closure of the polymeric structure and the overall reduction charge, when a negative potential sweep, as that represented by Figure 2, is considered. In other words, the charge consumed during reduction at potentials more cathodic than E_s will be considered as a reference value for the charge consumed for the opening of the polymeric structure along the conformational relaxation controlled oxidation. This ratio ranges between 0 at −900 mV and 0.36 at −3200 mV vs. SCE. Finally, the value λ/τ_0 was estimated as 1×10^5 cm s^{-1}. This corresponds to a rate of expansion of the conducting regions of 3×10^{-2} cm s^{-1} in a potential step from −2000 to 300 mV, in accordance with our observations.

When all those magnitudes are included in eq 36, a good agreement between experimental and simulated curves is achieved, as it is made clear when both types of curves are compared. The influence of the cathodic potential on the shape of theoretical chronoamperograms can be observed in Figure 3 (dashed lines). In the same form, the chronoamperometric responses to potentials steps from −2000 mV to different anodic limits are depicted by dashed lines in Figure 6. Chronoamperograms simulated for potential steps at different temperatures, the polymer being reduced at room temperature in all cases, can be observed in Figure 7. Both theoretical curves and the position of the chronoamperometric maxima are in accordance to experimental curves depicted by solid lines on the same figures. In order to translate this good agreement between theoretical and experimental curves into quantitative relationships, both experimental times and currents for the chronoamperometric maxima were plotted against theoretical values in Figures 10 and 11, respectively. Results point to a very good correlation for all the studied variables. Correlations are not so good when only eq 22 (that is, considering that all the oxidation charge is employed to open the polymeric network)

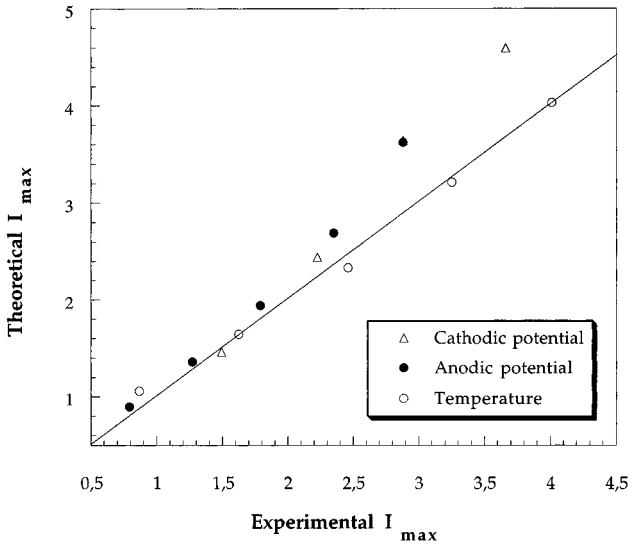

Figure 10. Correlation between theoretical and experimental values for the times of the chronoamperometric maxima, at different cathodic potentials of prepolarization, anodic potentials and temperatures. Data were extracted from figures 3, 6, and 7.

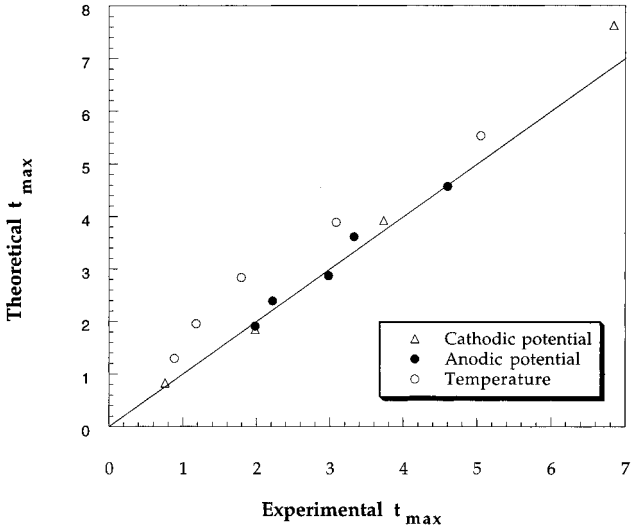

Figure 11. Correlation between theoretical and experimental values for the intensity maxima of the chronoamperometric curves. Data were extracted from figures 3, 6, and 7, respectively.

was considered, as shown in Figure 12: experimental and theoretical values for the intensities of the maxima are in clear disagreement, particularly when slow relaxation processes are present (high cathodic potentials, low anodic potentials, or low temperatures). This behavior can be explained when theoretical oxidation curves are decomposed in their relaxational and diffusional components (see Figure 13). The relaxation curve describes the initial slope of the curve, and it is responsible for the time at which the chronoamperogram reaches its maximum, whereas the diffusion curve approaches well to the shape of the chronoamperogram. Hence the intensity of the chronoamperometric maximum is better described by the diffusion component than by the relaxation component.

6. Conclusions

A simplified model for the oxidation of conducting polymers (transition from a neutral to an oxidized state) under conformational relaxation control was presented, able to explain both electrochemical responses and structural changes associated to those redox processes. The definition of a characteristic feature

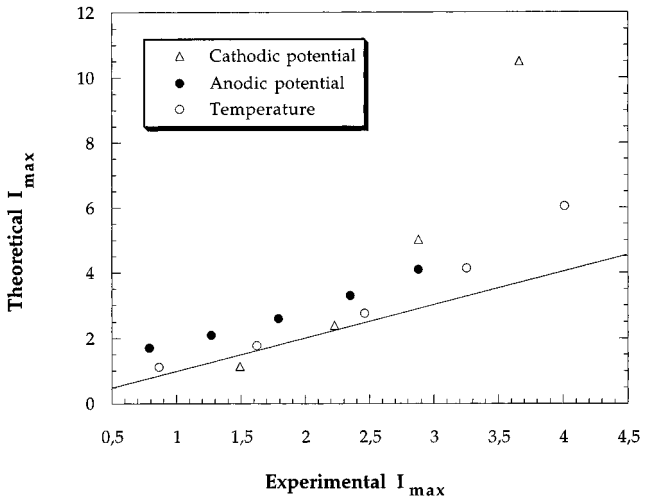

Figure 12. Correlation between theoretical and experimental values for the intensity maxima of the chronoamperometric curves. Experimental data were extracted from figures 3, 6, and 7, and theoretical results correspond to eq 22.

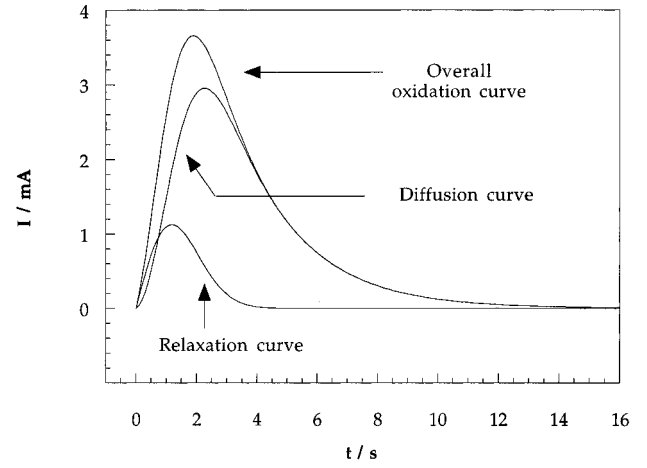

Figure 13. Separation of the overall oxidation curve into its two components: a relaxation curve, responsible for the initial slope and the position of the chronoamperometric maximum, and a diffusion curve which controls the overall shape of the chronoamperogram.

of the polymer as the conformational relaxation time allows the integration of polymer science and electrochemistry. The energy available to the polymeric chains to undergo conformational changes at constant temperature has been related to cathodic overvoltages, which control the compactness of the polymeric structure attained along reduction, and to anodic overvoltages, which are connected with the electrochemical work applied to the structure along its opening.

This is an open model, where physical and chemical magnitudes of the polymer/solvent/electrolyte system are implicit and need to be defined in subsequent improvements of the model. Polymer−polymer, polymer−solvent, and polymer−ion interactions in both neutral or oxidized states of the polymer must be quantified in future revisions. In the same form, magnitudes linked to the polymer structure, like the degree of cross-linking, or parameters linked to the interchain free volume, which depends on the redox state of the polymer, will be also included in the model. In spite of the present oversimplification, experimental chronoamperograms obtained under the influence of different electrochemical variables are simulated through the model with a good fitting. Subsequent improvements of the model will be applied to the optimization of technological applications of conducting polymers (artificial muscles and nerves, intelligent membranes, batteries, etc.) and to the description of other electrochemical responses (cyclic voltammetry, impedance spectroscopy, chronocoulometry, etc.).

Acknowledgment. The authors thank the Spanish Ministerio de Educación y Ciencia and the Eusko Jaurlaritza/Gobierno Vasco for finnancial support.

References and Notes

(1) Bredas, J. L. In *Handbook of conducting polymers*; Skotheim, T. A., Ed.; Wiley: New York, 1986; p 859.
(2) Feldman, B. J.; Burgmayer P.; Murray, R. W. *J. Am. Chem. Soc.* **1985,** *107*, 872.
(3) Posey, F. A.; Morozumi, T. *J. Electrochem. Soc.* **1966**, *113*, 176.
(4) Aoki, K.; Tezuka, Y. *J. Electroanal. Chem.* **1989**, *267*, 55.
(5) Aoki, K.; Tezuka, Y.; Shinozaki, K.; Satoh, H. *J. Electrochem. Soc. Jpn.* **1989**, *57*, 397.
(6) Feldberg, S. W. *J. Am. Chem. Soc.* **1984,** *106*, 4671.
(7) Yeu, T.; Yin, K. M.; Carbajal, J.; White, R. E. *J. Electrochem. Soc.* **1991**, *138*, 2869.
(8) Yeu, T.; Nguyen, T. V.; White, E. *J. Electrochem. Soc.* **1988**, *135*, 1971.
(9) Kalaji, M.; Peter, L. M.; Abrantes, L. M.; Mesquita, J. C. *J. Electroanal. Chem.* **1989**, *274*, 289.
(10) Hillman, A. R.; Bruckenstein, S. *J. Chem. Soc., Faraday. Trans.* **1993**, *89(20)*, 3779.
(11) Kaplin, D. A.; Qutubuddin, S. *J. Electrochem. Soc.* **1993**, *140*, 3185.
(12) Otero, T. F.; Angulo, E. *Solid State Ionics* **1993**, *63*−65, 803.
(13) Odin, C.; Nechtschein, M. *Synth. Met.* **1993**, *55*−57, 1281.
(14) Odin, C.; Nechtschein, M. *Synth. Met.* **1993**, *55*−57, 1287.
(15) Odin, C.; Nechtschein, M. *Phys. Rev. Lett.* **1991**, *67(9)*, 1114.
(16) Inzelt, G.; Horányi, G.; Chambers, J. Q. *Electrochim. Acta* **1987**, *32*, 757.
(17) Inzelt, G.; Day, R. W.; Kinstle, J. F.; Chambers, J. Q. *J. Phys. Chem.* **1983**, *87*, 4592.
(18) Heinze, J.; Bilger, R.; Meerholz, K. *Ber. Bunsenges. Phys. Chem.* **1988**, *92*, 1266.
(19) Odin, C.; Nechtschein, M. *Synth. Met.* **1991**, *43*, 2943.
(20) Aoki, K.; Cao, J.; Hoshino, Y. *Electrochim. Acta* **1994**, *39*, 2291.
(21) Aoki, K. *J. Electroanal. Chem.* **1994**, *373*, 67.
(22) Sabatani, E.; Ticianelli, E; Redondo, A.; Rubinstein, I.; Rishpon, J.; Gottesfeld, S. *Synth. Met.* **1993**, *55*−57, 1293.
(23) Brédas, J. L.; Thémans, B.; Fripiat, J. G.; André, J. M.; Chance, R. R. *Phys. Rev. B* **1984**, *29*, 6761.
(24) Marque, P.; Roncali, J. *J. Phys. Chem.* **1990**, *94*, 8614.
(25) Yeu, T.; Yin, K.-M.; Carbajal, J.; White, R. E. *J. Electrochem. Soc.* **1991**, *138*, 2869.
(26) Qiu, Y.; Reynolds, J. R. *Pol. Eng. Sci.* **1991**, *31*, 6.
(27) Penner, R. M.: Van Dyke, L. S.; Martin, C. R. *J. Phys. Chem.* **1988**, *92*, 5274.
(28) Slama, M., Tanguy, J. *Synth. Met*. **1989**, *28*, C171.
(29) Otero, T. F.; Rodríguez, J. In *Intrinsically Conducting Polymers: An Emerging Technology*; Aldissi, M., Ed.; NATO ASI Series; Kluwer Academic Publishers: Boston, MA, 1993.
(30) John, R.; Wallace, G. G. *J. Electroanal. Chem.* **1993**, *354*, 145.
(31) Pei, Q.; Inganäs, O. *J. Phys. Chem.* **1992**, *96*, 10507.
(32) Pei, Q.; Inganäs, O. *J. Phys. Chem.* **1993**, *97*, 6034.
(33) Baker, C.; Qiu, Y.-J.; Reynolds, J. R. *J Phys. Chem.* **1991**, *95*, 4446.
(34) Chesher, D. A.; Christensen, P. A.; Hamnett, A. *J. Chem. Soc., Faraday Trans.* **1993**, *89*, 303.
(35) Elliot, M.; Kopetove, A.; Albery, W. J. *J. Phys. Chem.* **1991**, *95*, 1743.
(36) Otero, T. F.; Sansiñena J. M. *Bioelectrochem. Bioenerg.* **1995**, *38*, 411.
(37) Otero, T. F.; Angulo, E.; Rodríguez, J.; Santamaría, C. *J. Electroanal. Chem.* **1992**, *341*, 369.
(38) Otero, T. F.; Rodríguez, J.; Santamaría, C. *Mater. Res. Soc. Symp. Proc.* **1994**, *330*, 333.
(39) Otero, T. F.; Rodríguez, J.; Angulo, E.; Santamaría, C. *Synth. Met.* **1993**, *55*−57, 3713.
(40) Otero, T. F.; Sansiñena, J. M.; Grande, H.; Rodríguez, J. *Portug. Electrochim. Acta*, in press.
(41) Avrami, M. *J. Chem. Phys.* **1939**, *7*, 1103.
(42) Avrami, M. *J. Chem. Phys.* **1940**, *8*, 212.
(43) Avrami, M. *J. Chem. Phys.* **1941**,*9*, 177.
(44) Otero, T. F.; Grande, H.; Rodríguez, J. *J. Electroanal. Chem.* **1995**, *394*, 211.
(45) Otero, T. F.; Grande, H.; Rodríguez, J. *Synth. Met.* **1996**, *76 (1*−3), 293.
(46) Otero, T. F.; Grande, H. *J. Electroanal. Chem.*, in press.
(47) Tsai, E. W.; Pajkossy, T.; Rajeshwar, K.; Reynolds, J. R. *J. Phys. Chem.* **1988**, *92*, 3560.